JACS
JOURNAL OF THE AMERICAN CHEMICAL SOCIETY

ARTICLE

pubs.acs.org/JACS

Ab Initio Study of Key Branching Reactions in Biodiesel and Fischer−Tropsch Fuels

Alexander C. Davis and Joseph S. Francisco*

Department of Chemistry and Department of Earth and Atmospheric Science, Purdue University, West Lafayette, Indiana 47907-1393, United States

Supporting Information

ABSTRACT: Many biologically and Fischer−Tropsch synthesized fuels contain branched alkanes which, during their combustion and atmospheric oxidation mechanism, produce methylalkyl radicals. As a result, an accurate description of the chemistry of these species is essential to integrating these fuels into our energy systems. Even though branched alkanes make up roughly one-third of the compounds in gasoline and diesel fuels, both experimental and theoretical data on methylalkyl radicals and their reactions are scarce, especially for larger chain systems and combustion conditions. The present work investigates all the hydrogen migration reactions available to the *n*-methylprop-1-yl through *n*-methylhept-1-yl radicals, for $n = 2-6$, using the CBS-Q, G2, and G4 composite computational methods, over a wide temperature range. The resulting thermodynamic and kinetic parameters are used to determine the effect that the presence of the methyl group has on these important unimolecular, chain branching reactions, for the reactions involving not only a tertiary abstraction site but also all the primary and secondary sites. The activation energies of hydrogen migration reactions with the methyl group, either within or immediately outside the ring, are found to be roughly 0.8−1.6 kcal mol^{-1} lower in energy than expected on the basis of analogous reactions in *n*-alkyl radicals. An important implication of this result is that the current method of using rate parameters derived from *n*-alkyl radicals to predict the chain branching characteristics of methylated alkyl radicals significantly underpredicts the importance of these reactions in atmospheric and combustion processes. Discussion of a possible cause for this phenomenon and its effect on the overall combustion mechanism of branched hydrocarbons is presented. Of particular concern is that 2,2,4,4,6,8,8-heptamethylnonane, which is currently used to model branched alkanes in diesel fuel surrogates, is predicted to have a much lower activation energy, by as much as 3 kcal mol^{-1}, for the dominant, 1,5 H-migration reactions than for the same reaction in many of the less branched alkanes that it is meant to represent. Also, counter to the currently accepted theory, the 3-methylalk-1-yl radical 1,4 and 1,5 H-migrations involving the movement of a secondary hydrogen are found to have higher rate coefficients than the corresponding reactions involving a tertiary hydrogen. The results presented here have significant implications for future experimental, computational, and combustion modeling studies.

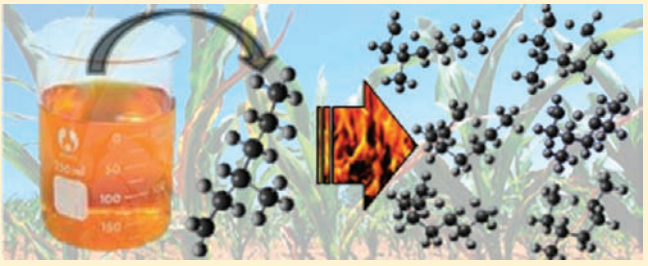

1. INTRODUCTION

Branched alkanes are a major component of traditional and many alternative fuel sources, including biodiesel and Fischer−Tropsch synthesized hydrocarbons.[1,2] With the rising demand for transportation fuels and the increasing concern about anthropogenically generated hydrocarbon pollutants, there is a growing need to better understand the fundamental processes that govern the combustion and atmospheric decomposition mechanisms of traditional and alternative fuels.[3] However, even for the simple hydrocarbons, such as methane or ethanol, the full combustion mechanism can contains hundreds of molecules and thousands of reactions.[4] Unfortunately, real fuels are complex mixtures of compounds that include *n*-alkanes, branched alkanes, cycloalkanes, and aromatic species (Figure 1).[3,5] To exacerbate matters, different types of fuel engine systems, such as diesel, spark ignition, and turbine jet engines, all require different fuel compositions with different combustion properties, as shown in Figure 1. Several studies have attempted to model traditional fuel combustion mechanisms using experimentally and computationally derived values to help to estimate unknown kinetic parameters.[4−8] However, even though branched alkanes represent 30−40% of the composition of diesel, gasoline, and jet fuels (Figure 1), very few experimental studies have reported on the chain branching reactions for this group of compounds, and those that have are very recent.[5,9−11] Instead, most studies focus on the mechanistically simpler *n*-alkanes, which make up only 5−20% of the components in traditional transportation fuels. An excellent review of hydrocarbon combustion modeling is provided by Simmie.[4]

At temperatures above 900 K, the combustion mechanisms of *n*-alkanes, branched alkanes, and other aliphatic hydrocarbons are dominated by unimolecular reactions, including β-bond scission and isomerization reactions.[6,10] Of particular interest

Received: June 14, 2011
Published: August 01, 2011

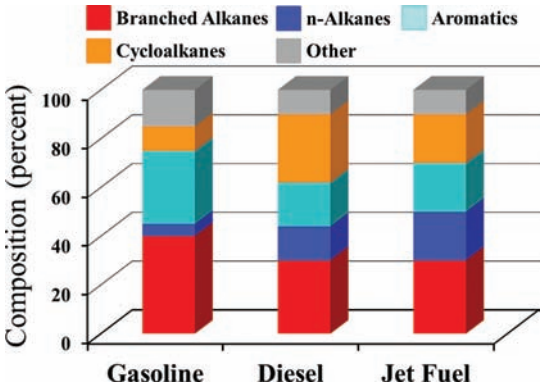

Figure 1. Composition of traditional transportation fuels arranged into categories based on structural similarities. Numbers are from ref 3.

are the unimolecular isomerization reactions involving the movement of a hydrogen atom, often termed H-migration. These reactions result in the relocation of the radical site and can lead to significant chain branching in the hydrocarbon combustion and atmospheric decomposition mechanisms. As such, the elucidation of their kinetic parameters enables an understanding of the composition and relative concentrations of the end products. These values can be determined through experimental, computational, and estimation methods.[12]

The experimental methods used for studying these unimolecular reactions involve the production of alkyl radicals through either photolysis[9,13−16] or pyrolysis.[10,12,17−22] The majority of the work on H-migration reactions in alkyl radicals has focused on straight chain *n*-alkyl radicals,[12−22] with only a few studies concentrating on branched alkyl radicals.[9−11] Tsang and coworkers reported evidence for 1,4 and 1,5 H-migrations in the unimolecular decomposition of 4-methylpent-1-yl and 5-methylhex-1-yl radicals, using single-pulse shock tube pyrolysis.[10,11] Watkins and O'Deen, investigating the decomposition of 3-methyl-1-buten-1-yl radicals produced by the photolysis of azoisopropane in the presence of acetylene, observed evidence of a 1,4 H-migration.[9] Due to the reactivity and short lifetimes of the intermediate species, individual rate parameters are inferred indirectly on the basis of the relative concentrations of the resulting products, using these methods. This makes it is difficult to distinguish between reactions that lead to the same product. It is for this reason that most studies utilize shorter alkyl chains, which contain fewer competing elementary reactions in their decomposition pathways. Also, in order to reduce the number of overlapping reactions, disfavored reaction paths, such as the 1,2 and 1,3 H-migrations, are commonly removed from consideration. The limited number of experimental studies above highlights the lack of kinetic information available in the literature on hydrocarbon systems that are essential to modeling real fuels.

Modern computational methods have enabled the determination of individual rate parameters in the combustion and atmospheric decomposition pathways of many alkyl radicals.[23−31] However, similar to their experimental counterparts, computational studies on branched alkyl radicals are limited in number.[30,32−34] Viskolcz et al. used the UHF/6-31G*//PM-SAC2/6-311G** level of theory to investigate the various H-migration reactions available to the 2-methylhexyl radical.[32] Barker and Ortiz, using the same system, performed master equation simulations.[33] Hayes and Burgess used the composite G3MP2B3 method for a large series of alkyl, allylic, and oxoallylic radicals to determine the barrier height of their respective H-atom transfers, but they only looked at the methylalkyl radicals in terms of their tertiary abstraction site and not the impact of the methyl group on other H-migration reactions.[30] Bankiewicz et al., using density functional theory (DFT), tried to evaluate an estimation method based on reaction classes for the 1,4 H-migrations using an array of alkyl radicals, some of which included methylalkyl radicals.[34] However, in their study, branched alkyl radicals were, again, only studied with regard to the tertiary hydrogen and not the effect of the methyl group on other reactions. In a recent review, Pitz and Mueller remarked that although a great deal of work has been done on determining kinetic parameters relevant to combustion systems in *n*-alkanes, the data set for branched alkanes is extremely limited, with only one system relevant to diesel fuels, 2,2,4,4,6,8,8-heptamethylnonane, having been studied both experimentally and with modeling work.[5]

Combustion models dealing with, as well as much of the discussion about, H-migrations rely on a conceptual model developed by Benson.[35] According to this model, the activation energy, E_a, can be predicted by summing the barrier height for a bimolecular hydrogen abstraction reaction, E_{abs}, between an alkane and alkyl radical, and the ring strain energy, E_{strain}, of an n+1 cycloalkane, where n is the number of carbon atoms in the ring structure of the H-migration transition state (eq 1):

$$E_a = E_{abs} + E_{strain} \quad (1)$$

Part of the reason for the continued popularity of this model is that when it was developed in the 1950s, it was able to predict the barrier heights for unknown reaction parameters in shorter alkyl radicals with reasonable accuracy and minimal effort. According to the n+1 cycloalkane model, the 1,5 H-migration, which has a six-member transition-state ring that is similar to cyclohexane, has the lowest barrier height and is the dominant reaction pathway. However, recent experimental and computational studies have reported that the 1,6 H-migration reactions activation energy is significantly less than predicted by Benson's model, making it a competitive pathway for heptyl and larger alkyl radicals.[12,21] Other computational studies have modified Benson's model to account for a possible relationship between reaction enthalpies and activation energies.[6,7,31] This, when combined with the variations in E_{abs} values for different hydrogen abstraction sites along branched and *n*-alkyl radical chains, leads to the prediction that tertiary abstraction sites will have lower barriers than the secondary sites, which should in turn be lower than those of the primary abstraction sites.

In each case, investigations into the effect of methyl substituents on alkyl chains are almost exclusively limited to the effect of abstraction from the tertiary position and do not consider the secondary effects that these methyl groups have on the stability of transition states when they are located within the ring structure. In both the 4-methylpent-1-yl and 5-methylhex-1-yl radical pyrolysis experiments, Tsang et al. reported that although they attempted to fit the 1,4 and 1,5 H-migration reaction rate parameters to the corresponding ones in their *n*-hexyl radical study, they were unable to do so without decreasing the activation energy for the methylated system by approximately 1 kcal mol^{-1}.[10,11] However, to date no discussion of the root cause of this lower than expected activation energy has been provided.

The work presented here investigates all of the H-migration reactions available to the *n*-methylprop-1-yl through *n*-methylhept-1-yl radical, for n = 2−6. This study attempts to assess the

effect that the methyl group has on the reaction enthalpy, activation energy, and rate coefficients of the 1,2 through 1,7 H-migration reactions. It also addresses the relative importance of the 1,5 and 1,6 H-migration reactions and the effect that the methyl group orientation (axial or equatorial) has on their rate coefficients over a wide range of temperatures. The observed trends reported in this study should enable the development of more accurate estimations of kinetic parameters for these important chain branching reactions, in not only the single-branched alkanes investigated in this study but also the longer and multibranched alkanes that make up a significant portion of both traditional and alternative transportation fuels.

2. COMPUTATIONAL METHODOLOGY

Hydrogen migration reactions are often described as an *a,b* H-migration, where *a* is the location of the initial radical site and *b* is the location of the abstraction site. Alternatively, other studies use an *Ncd* format, where *N* is the number of components in the ring of the transition state, including the hydrogen, and *c* and *d* are the types of radical sites (p = primary, s = secondary, and t = tertiary) for the product and reactant, respectively.[36] Following these methods, a 1,5 H-migration in 5-methyl-1-heptyl would be described as a 6tp reaction (Figure 2). This paper will utilize both methods to highlight different aspects of the isomerization reactions. However, in order to aid in the discussion of the methyl group location effect, a numerical subscript *n* will be added to the *Ncd* format to denote the location of the methyl group relative to the radical site in the reactant molecule, giving N_ncd. Also, on the basis of previous studies involving alkyl radicals, the secondary and tertiary sites will be sublabeled as either α or β depending on the location of the radical site relative to the end of the alkyl chain, when deemed appropriate. The symbol β will be used for all secondary sites that are two or more carbon groups away from a terminus. As a result, the above 5-methyl-1-heptyl radical 1,5 H-migration reaction will be indicated as $6_5t_\beta p$, whereas the same 1,5 H-migration in a 4-methyl-1-hexyl radical would be labeled $6_4s_\alpha p$. Finally, due to the significant 1,3 diaxial interactions that are present in methylcyclohexane, which is used as a model for the ring strain in the 1,5 and potentially 1,6 H-migration reactions, the methyl group in these reactions is placed in both the axial and equatorial positions (Figure 3) and will be labeled with either an A or E superscript, respectively. Thus, the 1,5 H-migration in the 4-methylhex-1-yl radical with the methyl group in an axial position will be labeled as $6_4{}^As_\alpha p$.

All geometry optimizations and frequency calculations for the reactants, products, and transition states are performed using the Gaussian 09 suite of programs. Each calculation is performed using the CBS-Q, G2, and G4 composite methods.[37] These computational methods are chosen for their high accuracies, having reported standard deviations of 1.1, 1.0, and 1.1 kcal mol^{-1}, respectively.[38,39] Transition states are confirmed by the presence of a single negative frequency that corresponds to the reaction path of the migrating hydrogen. Because the molecules of interest in this study involve both a radical site and a methyl group, virtually all reactants, products, and transition states will include at least one chiral center, the tertiary carbon. For transition states that involve a secondary abstraction site, an additional chiral site is introduced. This means that the selection of each of the two hydrogen atoms at a secondary abstraction site will result in slightly different activation energies. In order to minimize the interaction between the methyl and remaining branch, trans configurations were used for the 1,2 through 1,4 H-migration reactions. For the 1,5 and 1,6 reactions, which are predicted to be the primary reaction pathways, the remaining alkyl branch was placed in an equatorial position.[12] The methyl group, however, was placed in both axial and equatorial positions to help assess the effect that the methyl group position, relative to the abstraction site, has on the favorability of the H-migration reaction. Finally, for the 1,7 H-migration reactions, none of which includes a secondary abstraction site, the methyl group was placed in the equatorial position to minimize diaxial interactions in the transition state. The methods used to determine the

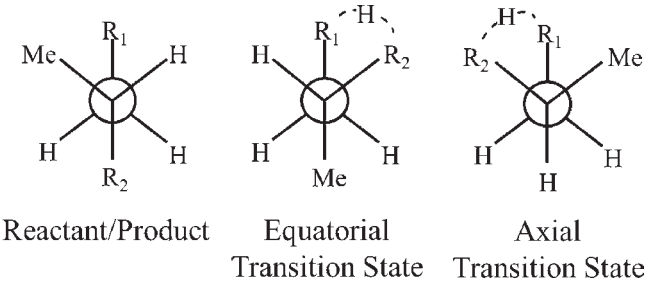

Figure 3. Newman projection of the location of the methyl group in the reactants/products and the axial and equatorial transition states.

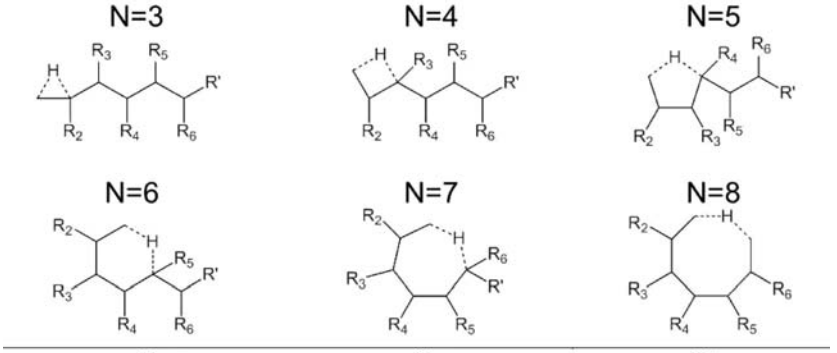

	N_npp		N_nsp		N_ntp	
N	Alkyl Chain Length	R_n=CH_3	Alkyl Chain Length	R_n=CH_3	Alkyl Chain Length	R_n=CH_3
3	n/a	n/a	R′=Butyl-Heptyl	n=3-6	R′=Propyl-Heptyl	n=2
4	R′=Propyl	n=2	R′=Butyl-Heptyl	n=2,4-6	R′=Butyl-Heptyl	n=3
5	R′=Butyl	n=2,3	R′=Pentyl-Heptyl	n=2,3,5,6	R′=Pentyl-Heptyl	n=4
6	R′=Pentyl	n=2-4	R′=Hexyl-Heptyl	n=2-4,6	R′=Hexyl-Heptyl	n=5
7	R′=Hexyl	n=2-5	R′=Heptyl	n=2-5	R′=Heptyl	n=6
8	R′=Heptyl	n=2-6	n/a	n/a	n/a	n/a

Figure 2. Nomenclature used in this study to describe the H-migration reactions.

tunneling contribution, *A*-factors, and overall rate constants have been described previously.[40] Frequencies and rotational constants are listed in Table S1 in the Supporting Information.

3. RESULTS AND DISCUSSION

3.1. Calibration of Computational Methods. Using the energies of 125 computationally determined reactions and comparing them to corresponding experimental values, Ochterski and co-workers and Curtiss et al. reported mean absolute deviations of 1.1, 1.0, and 0.8 kcal mol^{-1} for CBS-Q, G2, and G4, respectively.[38,41−43] Unfortunately, many of these reaction systems include molecules and reaction types that are different from the methylalkyl radical H-migrations reported here. In a previous study, seven reactions were used to assess the reliability of the CBS-Q, G2, and G4 methods for H-migrations in alkyl radicals, resulting in root mean squared (rms) deviations of 0.8, 0.9, and 0.6 kcal mol^{-1}, respectively.[12] However, none of these included a tertiary radical site; to remedy this, five reactions are shown in Table 1, the first three of which include methylalkyl radical. The resulting rms deviations are slightly larger than those for only alkyl radicals, with values of 1.0, 1.5, and 0.8 kcal mol^{-1}, respectively. Because the G4 method values are in the best agreement with the experimentally derived ones, the majority of the discussion in this paper will utilize the G4 data set.

The validity of the G4 method, and the methods used here for determining *A*-factor and tunneling coefficients, can be assessed by comparing the overall rate coefficients with theoretically and experimentally derived values from previous studies (Figure 4). The rate coefficients for the 1,4 H-migration reactions are in excellent agreement with the experimental results of McGivern et al. and Awan et al. but differ from the theoretical values of Barker et al. and Bankiewicz et al.[10,11,33,34] For the 1,5 H-migration reactions, there is again excellent agreement between the values presented here and the experimental work of McGivern et al. and Awan et al. for the 6_npp and 6_nsp reactions. The 6_5tp values, which involve the abstraction of a tertiary hydrogen, are in reasonable agreement with each other. The values of Barker et al. are significantly higher than either the values reported here or the previously mentioned experimental values.[33] Due to the good agreement between the G4 data set and previous experimental studies, we are confident the trends reported here represent an accurate description of the H-migration reactions present in the combustion and atmospheric decomposition mechanisms of methylated alkyl radicals.

3.2. Stability of Radical Sites in Methylalkyl Radicals. Previous studies that have looked at multiple H-migration reactions tend to treat all abstraction sites of a given type (i.e., primary, secondary, or tertiary) as having the same ΔH_{rxn} values.[30,31] This implies the underlying assumption that the stability of the radical site is only affected by substituents that are directly bound to the radical site. However, according to the group additivity values of Cohen and Sumathi et al., the stability of a radical site is also affected by those groups that are bound to its neighboring atoms.[44,45] Recent high-level computational work on *n*-alkyl radicals has confirmed that there is a consistent

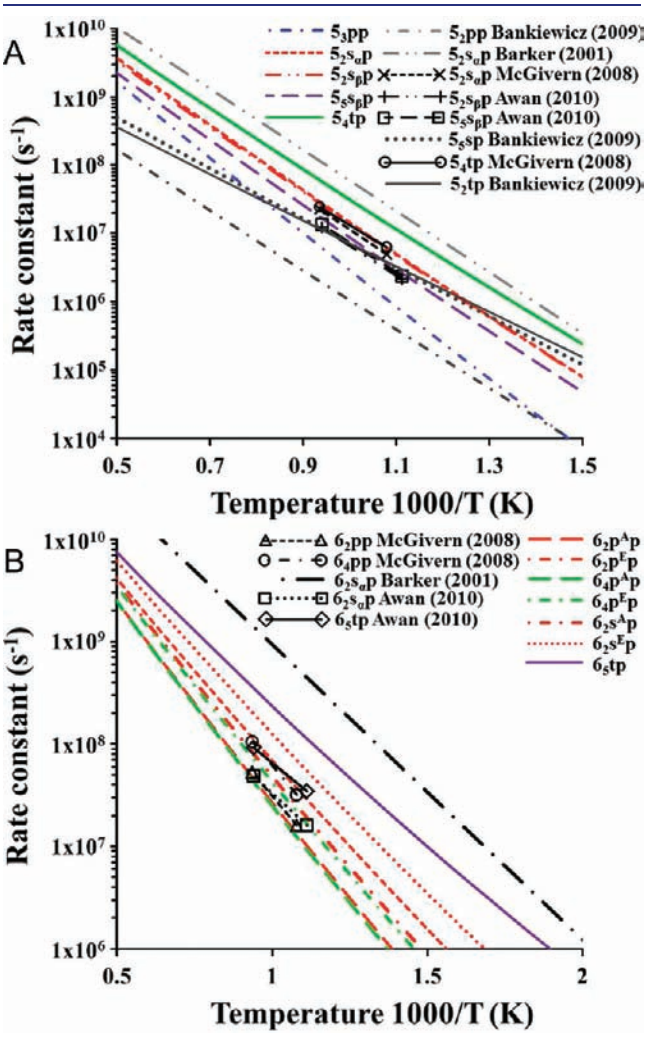

Figure 4. Comparison of the methylalk-1-yl radical 1,4 (A) and 1,5 (B) H-migration reaction rate coefficients calculated in this study (black lines and symbols) and those reported in other studies.[10113334]

Table 1. Comparison of Experimental ΔH°_{rxn} with Values Determined Using the Three Computational Methods Used in This Study (298 K)[50]

		ΔH°_{rxn} (kcal/mol)			
	reactions	exptl[50]	CBS-Q	G2	G4
(1)	$(CH_3)_2CHCH_2^\bullet \leftrightarrow (CH_3)_2{}^\bullet CCH_3$	−5.1 ± 0.7	−4.5	−4.5	−4.8
(2)	$(CH_3)_2{}^\bullet CCH_2CH_3 \leftrightarrow (CH_3)_2C{=}CH_2 + {}^\bullet CH_3$	23.9 ± 0.7	22	20.9	22.3
(3)	$^\bullet CH_3 + CH_2{=}CHCH_3 \leftrightarrow (CH_3)_2CHCH_2^\bullet$	−22.4 ± 0.6	−21.6	21	−21.9
(4)	$H + CH_3{}^\bullet CHCH_3 \leftrightarrow CH_3CH_2{}^\bullet + CH_3$	−9.6 ± 0.6	−9.8	−9.7	−9.9
(5)	$CH_4 + CH_3CH_2CH_2{}^\bullet \leftrightarrow CH_3CH_2CH_3 + {}^\bullet CH_3$	3.8 ± 0.5	2.8	4.2	3.8
		rmsd	1	1.5	0.8

Table 2. Thermochemical Data for Transition States of a Hydrogen Atom Migration across *n*-Methyl-1-alkyl Radical [Energies Are Relative to the Primary *n*-Methyl-1-alkyl Radical for Each Molecule at 0 K (kcal mol^{-1}); Values in Parentheses Are at 298 K]

		ΔH_{rxn}			$\Delta H^{\ddagger}$				
methylalkyl radical	rxn type	CBS-Q	G2	G4	CBS-Q	G2	G4	theor	exptl
				1,2 H-migration					
n = 2									
2-methylpropyl	$3_2t_\alpha p$	−4.7 (−4.5)	−4.7 (−4.5)	−5.0 (−4.8)	36.2 (36.1)	36.5 (36.3)	36.2 (36.0)	36.3[30]	
2-methylbutyl	$3_2t_\beta p$	−4.6 (−4.5)	−4.4 (−4.3)	−4.4 (−4.2)	35.8 (35.6)	36.3 (36.0)	36.2 (36.0)		
2-methylpentyl	$3_2t_\beta p$	−4.4 (−4.3)	−4.4 (−4.3)	−4.4 (−4.1)	36.3 (36.0)	36.2 (36.0)	36.2 (36.0)		
2-methylhexyl	$3_2t_\beta p$	−4.3 (−4.2)	−4.4 (−4.3)	−4.2 (−4.0)	36.5 (36.3)	36.3 (36.0)	36.2 (36.0)	36.8,[33] 36.5[32]	
2-methylheptyl	$3_2t_\beta p$	−3.8 (−3.7)	−4.4 (−4.3)	−4.3 (−4.0)	36.8(36.6)	36.2 (36.0)	36.2 (36.0)		
n = 3									
3-methylbutyl	$3_3s_\beta p$	−2.3 (−2.1)	−2.0 (−1.9)	−2.1 (−1.9)	38.0 (37.8)	38.5 (38.3)	38.4 (38.2)		
3-methylpentyl	$3_3s_\beta p$	−2.3 (−2.3)	−2.0 (−1.9)	−2.0 (−1.9)	37.9 (37.7)	38.5 (38.2)	38.4 (38.1)		
3-methylhexyl	$3_3s_\beta p$	−1.4 (−1.4)	−2.0 (−1.9)	−2.0 (−1.9)	38.8(38.6)	38.5 (38.2)	38.3 (38.1)		
3-methylheptyl	$3_3s_\beta p$	−0.9 (−0.8)	−2.0 (−1.9)	−2.0 (−1.9)	39.2 (39.0)	38.4 (38.2)	38.3 (38.1)		
n = 4									
4-methylpentyl	$3_4s_\beta p$	−2.9 (−2.9)	−2.9 (−3.0)	−3.1 (−3.1)	38.3 (38.0)	38.3 (38.0)	38.1 (37.8)		
4-methylhexyl	$3_4s_\beta p$	−3.4 (−3.4)	−3.2 (−3.2)	−3.4 (−3.4)	38.6 (38.3)	38.2 (37.8)	37.9 (37.5)		
4-methylheptyl	$3_4s_\beta p$	−3.3 (−3.7)	−3.2 (−3.2)	−3.3 (−3.4)	38.3 (38.0)	38.2 (37.8)	37.8 (37.5)		
n = 5									
5-methylhexyl	$3_5s_\beta p$	−2.9 (−2.9)	−2.3 (−2.3)	−2.8 (−2.8)	38.8 (38.5)	38.6 (38.4)	38.1 (37.8)	38.6[32]	
5-methylheptyl	$3_5s_\beta p$	−3.2 (−3.2)	−2.6 (−2.5)	−2.9 (−2.8)	39.0 (38.7)	38.5 (38.2)	38.1 (37.8)		
n = 6									
6-methylheptyl	$3_6s_\beta p$	−3.0 (−2.0)	−2.6 (−2.5)	−2.9 (−2.8)	38.4 (37.1)	38.3 (38.0)	38.1 (37.8)		
				1,3 H-migration					
n = 2									
2-methylpropyl	4_2pp	0.0 (0.0)	0.0 (0.0)	0.0 (0.0)	39.8 (39.5)	40.3 (40.0)	40.6 (40.2)		
2-methylbutyl	$4_2s_\alpha p$	−3.4 (−3.4)	−3.0 (−3.0)	−2.9 (−2.8)	37.1 (36.8)	37.9 (37.5)	38.4 (38.0)		
2-methylpentyl	$4_2s_\beta p$	−3.0 (−3.0)	−2.7 (−2.7)	−2.5 (−2.4)	36.9 (36.6)	37.6 (37.2)	38.1 (37.7)		
2-methylhexyl	$4_2s_\beta p$	−2.5 (−2.6)	−2.7 (−2.7)	−2.4 (−2.4)	36.6 (36.2)	37.6 (37.2)	38.1 (37.7)	38.3,[33] 38.1[32]	
2-methylheptyl	$4_2s_\beta p$	−3.2 (−3.1)	−2.7 (−2.7)	−2.3 (−2.4)	36.4 (36.0)	37.6 (37.2)	38.1 (37.7)		
n = 3									
3-methylbutyl	$4_3t_\alpha p$	−3.7 (−3.5)	−3.4 (−3.3)	−3.6 (−3.4)	36.8 (36.5)	37.3 (37.0)	37.3 (37.0)	37.5[30]	
3-methylpentyl	$4_3t_\beta p$	−3.2 (−3.1)	−2.9 (−2.8)	−3.4 (−3.3)	36.7 (36.4)	36.9 (36.5)	37.0 (36.6)		
3-methylhexyl	$4_3t_\beta p$	−1.5 (−1.4)	−3.1 (−3.0)	−3.7 (−3.6)	38.4 (38.0)	36.8 (36.4)	36.9 (36.5)		
3-methylheptyl	$4_3t_\beta p$	−1.1 (−1.0)	−3.0 (−3.0)	−3.7 (−3.6)	39.0 (38.6)	36.8 (36.4)	36.9 (36.5)		
n = 4									
4-methylpentyl	$4_4s_\beta p$	−2.6 (−2.5)	−2.2 (−2.2)	−2.2 (−2.2)	38.8 (38.4)	38.2 (37.7)	38.4 (38.0)		
4-methylhexyl	$4_4s_\beta p$	−2.5 (−2.5)	−2.4 (−2.4)	−2.5 (−2.5)	38.8 (38.4)	37.9 (37.4)	38.1 (37.6)		
4-methylheptyl	$4_4s_\beta p$	−3.9 (−3.9)	−2.4 (−2.4)	−2.5 (−2.5)	39.6 (39.1)	37.9 (37.4)	38.1 (37.5)		
n = 5									
5-methylhexyl	$4_5s_\beta p$	−2.3 (−2.3)	−2.5 (−2.6)	−2.9 (−3.0)	38.5 (38.1)	38.7 (38.3)	38.7 (38.2)	38.2[32]	
5-methylheptyl	$4_5s_\beta p$	−2.0 (−2.1)	−2.8 (−2.9)	−3.0 (−3.1)	39.0 (38.5)	38.5 (38.0)	38.1 (38.1)		
n = 6									
6-methylheptyl	$4_6s_\beta p$	−2.3 (−2.6)	−2.1 (−2.2)	−2.5 (−2.5)	37.2 (35.7)	38.6 (38.1)	38.7 (38.2)		
				1,4 H-migration					
n = 2									
2-methylbutyl	5_2pp	−0.9 (−1.0)	−1.0 (−1.0)	−0.8 (−0.8)	22.8 (22.0)	24.0 (23.1)	24.4 (23.6)		
2-methylpentyl	$5_2s_\alpha p$	−3.7 (−3.7)	−3.4 (−3.5)	−3.3 (−3.3)	20.7 (20.0)	21.9 (21.2)	22.4 (21.7)	28.3[34]	15.5[10]
2-methylhexyl	$5_2s_\beta p$	−3.2 (−3.3)	−3.1 (−3.1)	−2.9 (−3.0)	20.6 (19.9)	21.8 (21.0)	22.3 (21.5)	20.5,[33] 20.6[32]	16.1[11]
2-methylheptyl	$5_2s_\beta p$	−4.5 (−4.6)	−3.1 (−3.2)	−2.9 (−3.0)	18.8 (18.0)	21.7 (21.0)	22.3 (21.5)		
n = 3									
3-methylbutyl	5_3pp	0.9 (1.0)	1.0 (1.0)	0.8 (0.8)	23.8 (23.0)	24.9 (24.2)	25.8 (25.0)		

dx.doi.org/10.1021/ja205516s |*J. Am. Chem. Soc.* 2011, 133, 19110–19124

Table 2. Continued

		ΔH_{rxn}			$\Delta H^{\ddagger}$				
methylalkyl radical	rxn type	CBS-Q	G2	G4	CBS-Q	G2	G4	theor	exptl
3-methylpentyl	$5_3s_\alpha p$	−2.3 (−2.3)	−2.0 (−1.9)	−2.0 (−1.9)	20.5 (19.8)	22.1 (21.4)	22.3 (21.6)	25.0[34]	
3-methylhexyl	$5_3s_\beta p$	−1.6 (−1.6)	−1.7 (−1.6)	−1.6 (−1.6)	20.4 (19.7)	21.9 (21.2)	22.1 (21.4)		
3-methylheptyl	$5_3s_\beta p$	−3.0 (−3.0)	−1.7 (−1.7)	−1.6 (−1.6)	17.6 (16.9)	21.9 (21.2)	22.0 (21.3)		
n = 4									
4-methylpentyl	$5_4t_\alpha p$	−3.6 (−3.5)	−3.9 (−3.8)	−4.1 (−3.8)	21.3 (20.6)	20.9 (20.2)	21.0 (20.3)	21.2,[30] 23.8[34]	13.6[10]
4-methylhexyl	$5_4t_\beta p$	−2.4 (−2.4)	−3.8 (−3.8)	−4.5 (−4.5)	21.5 (20.7)	20.4 (19.6)	20.6 (19.8)	22.9[34]	12.0[48]
4-methylheptyl	$5_4t_\beta p$	−1.1 (−1.1)	−3.9 (−3.9)	−4.8 (−4.8)	23.1 (22.4)	20.3 (19.5)	20.4 (19.6)		
n = 5									
5-methylhexyl	$5_5s_\beta p$	−2.0 (−2.1)	−2.1 (−2.2)	−2.4 (−2.4)	22.2 (21.4)	22.5 (21.7)	22.5 (21.7)	21.5[32]	15.8[11]
5-methylheptyl	$5_5s_\beta p$	−3.4 (−3.4)	−2.4 (−2.4)	−2.5 (−2.5)	21.4 (20.6)	22.2 (21.4)	22.4 (21.5)		
n = 6									
6-methylheptyl	$5_6s_\beta p$	−3.5 (−4.6)	−2.7 (−2.8)	−2.9 (−3.0)	20.0 (18.2)	22.9 (22.1)	23.0 (22.2)		
				1,5 H-migration					
n = 2, axial									
2-methylpentyl	6_2pp	−0.8 (−0.8)	−0.5 (−0.5)	−0.2 (−0.2)	17.7 (16.7)	18.1 (17.1)	18.6 (17.5)		11.8[10]
2-methylhexyl	$6_2s_\alpha p$	−3.8 (−3.8)	−2.9 (−2.9)	−2.9 (−2.8)	15.8 (14.9)	16.2 (15.3)	16.8 (15.8)	13.2,[33] 13.4[32]	9.4[11]
2-methylheptyl	$6_2s_\beta p$	−3.3 (−3.3)	−2.5 (−2.6)	−2.5 (−2.5)	15.5 (14.5)	15.9 (14.9)	16.5 (15.5)		
n = 2, equatorial									
2-methylpentyl	6_2pp	−0.8 (−0.8)	−0.5 (−0.5)	−0.2 (−0.2)	16.6 (15.6)	17.3 (16.3)	17.8 (16.7)		11.8[10]
2-methylhexyl	$6_2s_\alpha p$	−3.8 (−3.8)	−2.9 (−2.9)	−2.9 (−2.8)	14.8 (13.9)	15.4 (14.5)	15.9 (14.9)	13.2,[33] 13.4[32]	9.4[11]
2-methylheptyl	$6_2s_\beta p$	−3.3 (−3.3)	−2.5 (−2.6)	−2.5 (−2.5)	14.2 (13.2)	15.2 (14.2)	15.6 (14.7)		
n = 3, axial									
3-methylpentyl	6_3pp	0.0 (0.0)	0.0 (0.0)	0.0 (0.0)	17.9 (16.9)	18.7 (17.6)	18.8 (17.8)		
3-methylhexyl	$6_3s_\alpha p$	−2.5 (−2.5)	−2.4 (−2.4)	−2.6 (−2.6)	17.4 (16.5)	16.8 (15.9)	16.9 (16.0)		13.0[48]
3-methylheptyl	$6_3s_\beta p$	−1.7 (−1.7)	−2.1 (−2.1)	−2.2 (−2.2)	17.1 (16.2)	16.5 (15.6)	16.6 (15.7)		
n = 3, equatorial									
3-methylpentyl	6_3pp	0.0 (0.0)	0.0 (0.0)	0.0 (0.0)	16.1 (15.2)	17.4 (16.5)	17.6 (16.6)		
3-methylhexyl	$6_3s_\alpha p$	−2.5 (−2.5)	−2.4 (−2.4)	−2.6 (−2.6)	14.6 (13.7)	15.5 (14.7)	15.6 (14.7)		13.0[48]
3-methylheptyl	$6_3s_\beta p$	−1.7 (−1.7)	−2.1 (−2.1)	−2.2 (−2.2)	14.0 (13.1)	15.3 (14.4)	15.3 (14.5)		
n = 4, axial									
4-methylpentyl	6_4pp	0.8 (0.8)	0.5 (0.5)	0.2 (0.2)	18.5 (17.5)	18.6 (17.6)	18.9 (17.8)		11.8[10]
4-methylhexyl	$6_4s_\alpha p$	−2.3 (−2.3)	−2.7 (−2.7)	−2.8 (−2.8)	16.7 (15.6)	16.9 (15.8)	17.0 (15.9)		
4-methylheptyl	$6_4s_\beta p$	−3.9 (−3.9)	−2.4 (−2.4)	−2.5 (−2.5)	17.4 (16.3)	16.6 (15.6)	16.7 (15.6)		
n = 4, equatorial									
4-methylpentyl	6_4pp	0.8 (0.8)	0.5 (0.5)	0.2 (0.2)	17.5 (16.5)	17.8 (16.8)	18.0 (17.0)		11.8[10]
4-methylhexyl	$6_4s_\alpha p$	−2.3 (−2.3)	−2.7 (−2.7)	−2.8 (−2.8)	14.4 (13.5)	15.0 (14.1)	15.0 (14.1)		
4-methylheptyl	$6_4s_\beta p$	−3.9 (−3.9)	−2.4 (−2.4)	−2.5 (−2.5)	14.2 (13.3)	14.7 (13.7)	14.7 (13.7)		
n = 5, tertiary									
5-methylhexyl	$6_5t_\alpha p$	−3.4 (−3.3)	−3.9 (−3.7)	−4.2 (−4.0)	15.3 (14.4)	14.3 (13.4)	14.0 (13.1)	12.1,[32] 14.5[30]	8.0[11]
5-methylheptyl	$6_5t_\beta p$	−1.4 (−1.4)	−3.7 (−3.7)	−4.5 (−4.5)	15.7 (14.7)	13.9 (12.9)	13.8 (12.8)		
n = 6, axial									
6-methylheptyl	$6_6s_\beta p$	−1.5 (−2.6)	−2.3 (−2.3)	−2.3 (−2.4)	16.5 (14.5)	16.2 (15.2)	16.4 (15.3)		
n = 6, equatorial									
6-methylheptyl	$6_6s_\beta p$	−1.5 (−2.6)	−2.3 (−2.3)	−2.3 (−2.4)	15.4 (13.4)	15.7 (14.7)	15.9 (14.8)		
				1,6 H-migration					
n = 2, axial									
2-methylhexyl	7_2pp	−1.0 (−0.9)	−0.6 (−0.6)	0.0 (0.0)	18.1 (16.9)	17.8 (16.6)	18.5 (17.2)	14.7,[33] 15.1[32]	
2-methylheptyl	$7_2s_\alpha p$	−4.0 (−4.0)	−3.0 (−2.9)	−2.9 (−2.8)	15.4 (14.3)	15.4 (14.3)	16.0 (14.9)		
n = 2, equatorial									
2-methylhexyl	7_2pp	−1.0 (−0.9)	−0.6 (−0.6)	0.0 (0.0)	16.9 (15.8)	17.1 (16.0)	17.7 (16.5)		
2-methylheptyl	$7_2s_\alpha p$	−4.0 (−4.0)	−3.0 (−2.9)	−2.9 (−2.8)	13.5 (12.5)	14.8 (13.8)	15.3 (14.3)		
n = 3, axial									

dx.doi.org/10.1021/ja205516s |*J. Am. Chem. Soc.* 2011, 133, 19110–19124

Table 2. Continued

		ΔH_{rxn}			$\Delta H^{\ddagger}$				
methylalkyl radical	rxn type	CBS-Q	G2	G4	CBS-Q	G2	G4	theor	exptl
3-methylhexyl	7_3pp	0.9 (0.9)	0.7 (0.8)	0.8 (0.9)	20.1 (19.0)	19.0 (17.8)	19.2 (18.0)		
3-methylheptyl	$7_3s_\alpha p$	−2.8 (−2.7)	−1.9 (−1.8)	−2.1 (−1.9)	17.6 (16.5)	16.7 (15.6)	16.8 (15.8)		
n = 3, equatorial									
3-methylhexyl	7_3pp	0.9 (0.9)	0.7 (0.8)	0.8 (0.9)	17.9 (16.8)	17.7 (16.5)	17.9 (16.8)		
3-methylheptyl	$7_3s_\alpha p$	−2.8 (−2.7)	−1.9 (−1.8)	−2.1 (−1.9)	15.3 (14.3)	15.4 (14.4)	15.6 (14.6)		
n = 4, axial									
4-methylhexyl	7_4pp	−0.9 (−0.9)	−0.7 (−0.8)	−0.8 (−0.9)	19.3 (18.0)	18.3 (17.0)	18.4 (17.1)		
4-methylheptyl	$7_4s_\alpha p$	−3.3 (−3.7)	−3.2 (−3.2)	−3.3 (−3.4)	17.9 (16.8)	16.0 (14.8)	16.2 (15.0)		
n = 4, equatorial									
4-methylhexyl	7_4pp	−0.9 (−0.9)	−0.7 (−0.8)	−0.8 (−0.9)	17.0 (15.9)	16.9 (15.8)	17.1 (15.9)		
4-methylheptyl	$7_4s_\alpha p$	−3.3 (−3.7)	−3.2 (−3.2)	−3.3 (−3.4)	13.6 (12.6)	14.6 (13.5)	14.7 (13.6)		
n = 5, axial									
5-methylhexyl	7_5pp	1.0 (0.9)	0.6 (0.6)	0.0 (0.0)	19.1 (17.9)	18.4 (17.2)	18.5 (17.2)		
5-methylheptyl	$7_5s_\alpha p$	−1.2 (−1.2)	−2.7 (−2.7)	−2.8 (−2.8)	16.8 (15.6)	16.1 (14.9)	16.1 (14.9)		
n = 5, equatorial									
5-methylhexyl	7_5pp	1.0 (0.9)	0.6 (0.6)	0.0 (0.0)	17.9 (16.7)	17.7 (16.6)	17.7 (16.5)	15.3[32]	
5-methylheptyl	$7_5s_\alpha p$	−1.2 (−1.2)	−2.7 (−2.7)	−2.8 (−2.8)	15.0 (13.9)	14.9 (13.8)	15.0 (13.9)		
n = 6, tertiary									
6-methylheptyl	$7_6t_\alpha p$	−2.8 (−3.7)	−4.0 (−3.9)	−4.3 (−4.0)	15.2 (13.2)	13.7 (12.7)	13.6 (12.6)	14.1[30]	
				1,7 H-migration					
n = 2									
2-methylheptyl	8_2pp	−1.0 (−1.0)	−0.4 (−0.4)	0.0 (0.0)	20.4 (19.1)	20.3 (19.0)	20.9 (19.6)		
n = 3									
3-methylheptyl	8_3pp	0.4 (0.4)	0.7 (0.8)	0.8 (0.9)	22.2 (20.9)	20.7 (19.5)	21.1 (19.8)		
n = 4									
4-methylheptyl	8_4pp	0.0 (0.0)	0.0 (0.0)	0.0 (0.0)	22.8 (21.5)	20.0 (18.7)	20.3 (18.8)		
n = 5									
5-methylheptyl	8_5pp	−0.4 (−0.4)	−0.7 (−0.8)	−0.8 (−0.9)	21.9 (20.6)	20.0 (18.7)	20.3 (18.9)		
n = 6									
6-methylheptyl	8_6pp	1.0 (0.0)	0.4 (0.4)	0.0 (0.0)	21.4 (19.1)	20.6 (19.4)	20.9 (19.6)		

difference in product stability between H-migrations involving a secondary site that is adjacent to the terminal carbon, *N*s$_\alpha$p, and the nonterminal adjacent secondary site, *N*s$_\beta$p.[12] In *n*-alkyl radicals, these s$_\alpha$ sites are 2.5−2.6, 2.4, and 2.5−2.9 kcal mol^{-1} more stable than a primary radical site for the G4, G2, and CBS-Q methods, respectively. Moving the radical farther away from the terminal carbon, giving the s$_\beta$ sites, destabilized the radical site by approximately 0.4, 0.5, and 0.0−0.6 kcal mol^{-1}, resulting in ΔH_{rxn} values for the *N*s$_\beta$p of −2.1 to −2.2, −2.0 to −2.1, and −1.9 to −3.4 kcal mol^{-1} for G4, G2, and CBS-Q methods, respectively. The large range of values for the CBS-Q method is attributed to a size-based error which increases with the length of the carbon chain.[12,40] Evidence for a similar error is observed in the data presented here, and this error leads to differences in ΔH_{rxn} values of up to 3.7 kcal mol^{-1} between the CBS-Q and the G2 and G4 data sets (Table 2).

For methylalkyl radicals, the treatment of all primary, secondary, and tertiary radical sites as equivalent will lead to significant errors in the perceived stability of these sites, resulting in inaccurate ΔH_{rxn} values for the H-migration reactions. Figure 5 and the ΔH_{rxn} values in Table 2 clearly show that, as expected, the tertiary radicals are the most stable, with the N$_{N-1}$tp

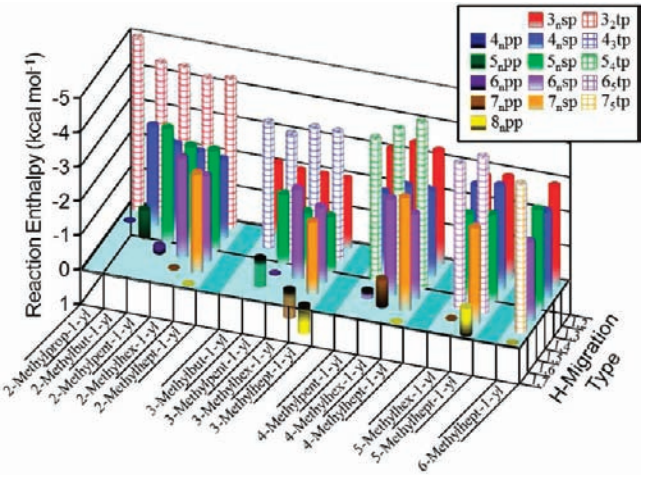

Figure 5. Plot of the G4 enthalpy of reactions for the H-migrations for each *n*-methylalk-1-yl radical (at 0 K). The *N*$_n$pp, *N*$_n$sp, and *N*$_{N-1}$tp reactions are indicated by darker, lighter, and fill patterns of the same color for a given *N*. The vertical axis is reversed to allow for easier visualization of the results.

reactions having the most exothermic reaction enthalpies, followed by the secondary and then the primary radicals. If the stability of the radical site were dependent solely on the substituents bound directly to the radical site, or if a methyl group bound to an adjacent carbon had no effect, then the values for all tertiary sites would be the same, as would all the secondary and primary reactions. However, this is not the case, as can clearly be seen in Figure 5. For the $N_n$pp reactions, there are three H-migrations for which the reactants are the same as the products: the 4_2pp, 6_3pp, and 8_4pp reactions in 2-methylpropyl, 3-methylbutyl, and 4-methylheptyl radicals, respectively, making them thermoneutral. The rest of the $N_n$pp reactions show differences in stability between the reactants and products. Although the G4 and G2 data sets are generally in excellent agreement, they do show some differences in the relative stabilities of the 2-methyl- versus 5-methylhex-1-yl, and of the 2-methyl- versus 6-methylhept-1-yl radicals. The G4 data set reports both sites in each set as being equally stable, whereas both the G2 and CBS-Q data sets show the 2-methylalk-1-yl radicals as being less stable by ~0.5 and 1 kcal mol^{-1}, respectively. The G2 and CBS-Q values for the 2-methylhexyl and 2-methylhept-1-yl are also consistent with the values for the 2-methylbut-1-yl and 2-methylpent-1-yl for all three computational methods used in this study. Due to the agreement with two of the three composite methods used in this study, along with the trends for the smaller 2-methylalkyl radical for the G4, it is likely that the discrepancy is due to some artifact of the G4 method. For the methylalkyl radicals, similar to the *n*-alkyl radicals, the presence of the methyl group on the α-carbon causes ~0.4−0.8 kcal mol^{-1} of instability. This is why the N_2pp reactions consistently have exothermic ΔH_{rxn}, and the N_{N-2}pp reactions are always endothermic (Table 2 and Figure 2). In the former the radical site moves away from the methyl group, and in the latter it moves next to the methyl group. The radical sites also appear to be stabilized by the presence of a methyl group in the *β*-position, as is evidenced by the endothermic ΔH_{rxn} for the 7_3pp and 8_3pp reactions.

As with the *n*-alkyl radical *N*sp reactions, the secondary radical sites that are adjacent to a terminal carbon, the $N_n s_\alpha p$ products, are 0.3−0.4 kcal mol^{-1} more stable than the secondary sites that are not directly adjacent to a terminal carbon, the $N_n s_\beta p$ products. Similar to the $N_n$pp reactions, a methyl group on the carbon adjacent to a secondary radical site, the result of the N_{N-2}sp and $N_n$sp reactions, also causes ~0.4 kcal mol^{-1} of instability. The branched methyl group in the *β*-position also appears to stabilize a secondary radical site by ~0.4 kcal mol^{-1}, corresponding to the N_{N-3}sp and N_{N+1}sp. This last effect is likely the result of a reduction in gauche interactions between the methyl group and the secondary radical site.

All of the above stabilizing/destabilizing trends result in a significant range of ΔH_{rxn} values for the $N_n$pp, $N_n$sp, and N_{N-1}tp reactions. Although most of the individual values are within the rms deviation reported above for the G4 method, the facts that they are also observed in the G2 method, and that both the G4 and G2 methods have similar and consistent values for all systems, suggest they are real. For all the H-migrations, the 2-methylalk-1-yl radicals have the most exothermic ΔH_{rxn} values, which results from the instability of having the methyl group next to the initial radical site. Similarly, the 3-methylalk-1-yl reactions are the least exothermic, with three of the four N_3pp reactions being endothermic; the remaining one is the 6_3pp, in which the reactants and products are identical. The remaining *n*-methylalk-1-yl radical H-migration reactions all have similar ΔH_{rxn} values, though each is modified by the trends in stability of the radical site described above. The variations in radical site stability affect not only the thermodynamic favorability of the H-migration reaction but also, as will be seen in the next section, the activation energy barriers and hence the kinetic favorability. Although each individual stabilizing effect reported above is relatively small, when there are multiple methyl groups the overall effect can be fairly large. Based on the above values, fuels with methyl groups at the 2 and 4 positions, such as the 2,2,4,4,6,8,8-heptamethylnon-1-yl, which is used as a surrogate for diesel fuel studies, should be more susceptible to 1,6 H-migration reactions, with ΔH_{rxn} values up to 2.0 kcal mol^{-1} lower than would be observed for 6-methylnon-1-yl radical. At the same time, 1,5 H-migration in the same surrogate fuel would only be 0.4 kcal mol^{-1} lower than that of the single methylated, 6-methylnon-1-yl radical.

3.3. Activation Energies. Similar to the ΔH_{rxn} values, a significant variation in the barrier heights for each set of 1,*n* H-migration reactions is observed (Figure 6 and Table 2). As expected, those reactions involving the migration of a tertiary hydrogen have the lowest activation energy and will therefore have the highest reaction rates. What is unexpected, however, is that the activation energies for the $N_n$pp and $N_n$sp reactions in methylalkyl radicals are often significantly less than is observed for the *n*-alkyl radicals.[12] A possible explanation for this comes from observing the shift in the methyl group between gauche and anti configurations in the reactants, products, and transition-state species (Figure 3). In the reactants and products, the methyl group produces a gauche interaction, which adds approximately 0.8 kcal mol^{-1} per interaction.[46] When the alkyl chain rearranges itself to form the transition state, the chain itself goes from anti to gauche configurations, leading to approximately 0.8 kcal mol^{-1} of ring strain per shift, though this value will be higher for the smaller transition states (with C−C−C−C dihedral angles of less than 60°). For methylated alkyl radicals, however, the introduction of ring strain from these new gauche interactions will be partially negated by a corresponding shift of the methyl group from the gauche to anti position. The effect of this can be seen in the activation energies of the various H-migration reactions (Figure 6).

Although both the 1,2 and 1,3 H-migration reactions, due to their high activation energy barriers, are not expected to contribute meaningfully to the overall atmospheric decomposition and combustion mechanisms for methylated hydrocarbons, their barrier heights do yield information about the extent to which methyl groups affect the activation energies of H-migration reactions for methyl groups that are outside the ring portion of the transition state. For the 1,2 H-migrations, the transition state contains only two carbons, thus there is no location for the methyl group to exist within the ring structure, and the rearrangement of the molecule into the transition state does not introduce any new gauche interactions. As a result, the activation energies for the $2_n s_\alpha p$ reactions are all very similar to the barrier heights for their corresponding unmethylated counterparts. However, for the 1,3 H-migration reactions (Figure 6B), the methyl group can be located within the ring structure of the transition state, 4_2pp and 4_2sp. For the butyl through heptyl radicals, the activation energies of the 4_2sp reactions are all approximately 1 kcal mol^{-1} lower than the values for the corresponding *n*-alkyl radicals, which is well predicted by the 0.8 kcal mol^{-1} of a single gauche interaction and the instability of the of 2-methylalk-1-yl radicals. Because the H-migration transition states resemble cycloalkanes, methyl groups adjacent to the

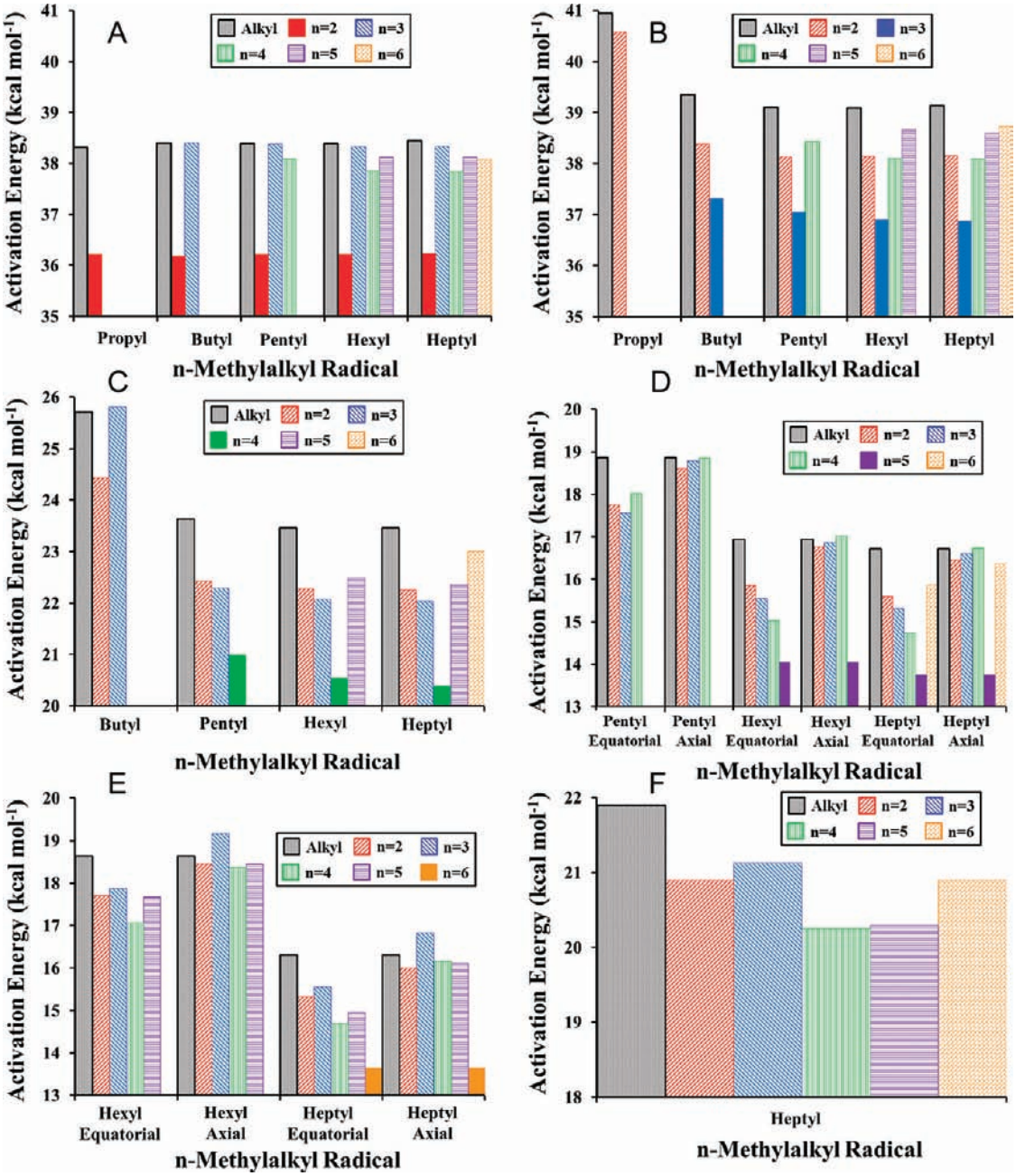

Figure 6. Bar graph of the G4 data set activation energies of the (A) 1,2, (B) 1,3, (C) 1,4, (D) 1,5, (E) 1,6, and (F) 1,7 H-migration reactions. Solid fill indicates an Ntp reaction.

abstraction site ($N_n$sp) will also have anti/gauche interactions with the migrating hydrogen and the ring structures, making the 4_4sp barrier heights also roughly 1.0 kcal mol^{-1} less than the *n*-alkyl 4sp values. The lower than expected value for the $4_5s_\beta p$ seen in the heptyl is likely the result of the increased stability of the radical at the abstraction site relative to its reactant position, as mentioned in the previous section. For both the 1,2 and 1,3 H-migration reactions, the variations observed in the activation energies and the ΔH_{rxn} values follow an Evans−Polanyi relationship (eq 2 and Figure 7), with R^2 values of 0.87 and 0.85, respectively.[47]

$$E_a = a\Delta H_{rxn} + b \quad (2)$$

where *a* and *b* are fitted parameters for each reaction class. For the larger transition states, the variations between activation energy and reaction enthalpy are not as clear.

Expanding the transition-state ring size by another carbon, resulting in the 1,4 H-migration reactions, causes a significant reduction in the activation energies, which is similar to the trends observed for *n*-alkyl radicals. As with the 1,2 and 1,3 H-migration reactions, the activation energies for the 1,4 H-migration reactions are significantly lower than their *n*-alkyl counterparts (Figure 6C). For this reaction group there are two positions for the methyl group that are within the transition-state ring, corresponding to the 5_2pp, 5_2sp, 5_3pp, and 5_3sp reactions. The 5_2pp, 5_2sp, and 5_3sp reactions all have activation energies that are

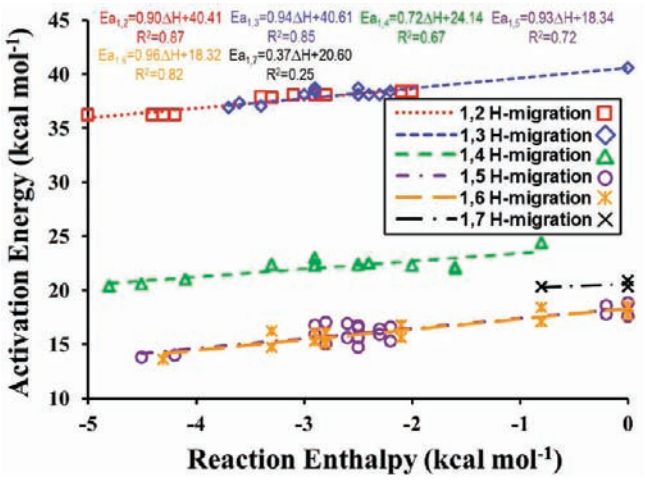

Figure 7. Evans–Polanyi plot of activation energies versus reaction enthalpies for the *n*-methylalk-1-yl radical H-migration reactions.

approximately 1.2–1.5 kcal mol^{-1} lower than their *n*-alkyl radical counterparts. For the 5_2sp reaction, these values correspond well to the summation of the 0.4–0.8 kcal mol^{-1} difference in stability between the 2-methyl and 4-methylalk-1-yl radicals, and the 0.8 kcal mol^{-1} gauche-to-anti configuration shift of the methyl group. For the 5_3sp reactions, one would expect a 1.6 kcal mol^{-1} reduction in barrier height compared to the alkyl radical systems, based on the two gauche interactions in the reactant. However, some of this effect is diminished by the instability caused by the presence of the radical site next to the methyl group, which ranges between 0.4 and 0.8 kcal mol^{-1} for the 5_3pp and 5_3sp reactions. The one seemingly aberrant data point, the 5_3pp activation energy, is actually higher than its butyl 5pp counterpart. The reason for the large differences in the 5_3pp energy is that the reactant methyl group only has one gauche interaction, giving it only 0.8 kcal mol^{-1} barrier height reduction instead of the 1.6 kcal mol^{-1} present in the 5_3sp. The 5_5sp activation energies are also significantly lower than those of the unbranched systems, which, similar to the 1,3 H-migration reactions, is likely due to the gauche interaction between the remaining chain and the transition-state ring. The 5_6sp reaction for the 6-methylhept-1-yl radical also has a lower barrier height than the heptyl radical 4sp, by 0.5 kcal mol^{-1}, which is similar to the trends seen in the 1,3 H-migrations for the N_{N+1}sp and N_{N+2}sp reactions. Finally, the 5_4tp reactions have activation energies that are lower than those of either their 5sp alkyl or 5_nsp methylalkyl counterparts by 2.6–3.1 and 1.3–2.6 kcal mol^{-1}, respectively. As a result, the 5_4tp reactions are expected to have significantly higher rate coefficients than their 5_nsp and 5_npp counterparts and may even be competitive with the 1,5 and 1,6 H-migrations for 4-methylpent-1-yl and larger radicals. Unfortunately, due to the complex interplay of stabilizing and destabilizing interactions within the 1,4 H-migrations, the relationship between activation energies and reaction enthalpies is not well described by the Evans–Polanyi relationship (Figure 7), giving an R^2 value of 0.67. This divergence will make the development of automated reaction mechanism software difficult for methylalkanes.

The next-largest transition states, the 1,5 H-migration reactions, have the second lowest barrier heights and, on the basis of their higher *A*-factors, are expected to be the predominant unimolecular chain branching reactions for pentyl and longer methylalkyl radicals (Table 2 and Figure 6D). Previous experimental work on branched alkyl radicals, reported by McGivern et al. and Awan et al., demonstrated that the 1,5 H-migration reactions have lower barrier heights than the 1,4 H-migrations, even for the 5_4tp versus the 6_4sp reaction.[10,11] However, Larson et al. suggest that the 5_4tp will have the lower barrier height.[48] The CBS-Q, G2, and G4 data sets all agree with the former assertion. A comparison of the activation energies reported here with previous literature values (Table 2) shows an excellent agreement with the high-level G3MP2B3 values of Hayes and Burgess, and reasonable agreement with the lower level calculations of Viskolcz et al. and Barker and Ortiz.[30,32,33] Although there appears to be a significant difference between the theoretical and experimental activation energy values reported by Tsang and co-workers, the determined rate coefficients for the temperature range at which the shock tube studies were conducted are in excellent agreement (Figure 4B) with the values reported here.[10,11] The transition-state ring of the 1,5 H-migration reactions has three locations within the ring structure for the methyl group, corresponding to the 6_2pp through the 6_4sp reactions. On the basis of the reaction enthalpies, one would expect the barrier heights for the 6_npp reactions to all be similar, with the 6_2pp reaction being the lowest and the 6_4pp reaction being the highest. However, if the methyl group is in an equatorial position within the transition-state ring, the 6_3^Epp reaction has the lowest activation energy. As is expected, the 6_5tp reactions have the lowest activation energies; however, surprisingly, the 6_4^Esp barrier height reduces from 18.0 to 15.0 kcal mol^{-1}, making it only 1 kcal mol^{-1} higher than the barrier height for the 6_5tp reaction. The activation energeis of both the 6_2^Esp and 6_3^Esp reactions are significantly lower than those of their 6_npp counterparts, reducing by 1.9 and 2.0 kcal mol^{-1}, respectively; however, they are also 0.9 and 0.6 kcal mol^{-1} higher than for the 6_4^Epp. In each case, the 6_n^Epp and 6_n^Esp reactions are between 1.0 and 2.4 kcal mol^{-1} lower than their alkyl radical counterparts. This difference can again be correlated to the shift of the methyl group from a gauche to an anti configuration (Figure 3). Due to the complexity of the multiple interactions present in the transition state, the correlation between activation energies and reaction enthalpies is not well described by an Evans–Polyani relationship, which has an R^2 value of 0.72 (eq 2 and Figure 7).[47]

Similar to the *n*-alkyl radical system, the methylalkyl radical 1,6 H-migrations tend to have lower activation energies than their equivalent methylalkyl 1,5 reactions; e.g., the 7_npp reactions are lower than the 6_npp. This is not to say that the 1,6 H-migration barrier heights for all *n*-methylalkyl radicals are lower than the 1,5 counterparts. For example, in 4-methylhexane the $6_4^E s_\alpha p$ reactions have an activation energy that is ~2.1 kcal mol^{-1} lower than the 7_4^Epp reactions. However, the 6_4^Epp activation energy is 0.9 kcal mol^{-1} higher than that of the 7_4^Epp reaction. As a result, studies that use *n*-methylhexyl or shorter radicals should not be used to predict the relative importance of the 1,5 versus 1,6 H-migration reaction pathways for *n*-methylheptyl or larger radicals. A comparison of H-migrations involving similar abstraction sites shows that the 7_npp activation energies are 0.1–0.9 kcal mol^{-1} lower than those for the 6_npp reactions, except for the N_3^Epp, in which the 7_3^Epp reaction activatoin energy is 0.3 kcal mol^{-1} higher than that of the 6_3^Epp. The $7_n s_\alpha p$ reactions also tend to have lower barrier heights than the $6_n^E s_\alpha p$ reactions by between 0.0 and 0.6 kcal mol^{-1}. However, because the $6_n s_\beta p$ activation energies are 0.3 kcal mol^{-1} lower than those of the

$6_n s_\alpha p$ reactions, the *n*-methylheptyl $7_n s_\alpha p$ reactions are less competitive with their $6_n s_\beta p$ counterparts than the $7_n s_\beta p$ and $6_n s_\beta p$ should be in the methyloctyl radicals.

Within the 1,6 H-migration reaction group there are significant variations in the activation energies. These reactions contain four locations for the methyl group within the transition-state ring, corresponding to the 7_2pp through 7_5sp reactions. For the equatorial arrangements, the 7_2^Epp and 7_5^Epp activation energies are both 1.1 kcal mol^{-1} less than for the *n*-alkyl 7pp, which is in agreement with the 0.8 kcal mol^{-1} predicted by the previous gauche/anti conformation argument. Similarly, 7_3^Epp activation energy should also be approximately 0.8 kcal mol^{-1} less than that of the alkyl 7pp reaction due to the summation of the 0.8 kcal mol^{-1} reaction enthalpy and the 1.6 kcal mol^{-1} barrier height reduction from the gauche/anti effect, which agrees with the observed 0.7 kcal mol^{-1} difference. On the other hand, the 7_4^Epp arrangement is only 1.5 kcal mol^{-1} less than that of the alkyl 7pp, instead of the 2.4 kcal mol^{-1} predicted by the summation of the anti/gauche effect and the −0.8 kcal mol^{-1} ΔH_{rxn}. Elongation of the chain, resulting in 7_n^Esp reactions, reduces the activation energy of each reaction, except the 7_5^Esp, by roughly 2.3 kcal mol^{-1}. In the case of the 7_5^Esp, the barrier height decreases by an additional 0.4 kcal mol^{-1}, which can be attributed to the new gauche/anti effect introduced by the alkyl chain extending from the ring at the abstraction site. As with the previous systems, the tertiary abstraction site, 7_6tp, has the lowest barrier of the H-migration group, being 1.1 kcal mol^{-1} less than that of the 7_4sp. It should be noted that the 7_6tp activation energy is also 2.3 kcal mol^{-1} less than in the 6_6sp reaction, suggesting that under certain reaction conditions the 7_6tp may become the dominant reaction pathway for the 6-methylheptyl and longer radicals. As with the 1,5 H-migration reactions, the significant number of counteracting stabilizing effects diminishes the correlation between activation energy and reaction enthalpy, giving an R^2 value of 0.82 (eq 2 and Figure 7).

The last set of H-migrations investigated in this study are the 1,7 H-migrations. The transition-state ring structure has five locations for the methyl group to occupy, which result in the 8_2pp through 8_6pp reactions. Since this study is limited to the *n*-methylpropyl through *n*-methylheptyl radicals, the 1,7 H-migration reactions presented here include only the primary−primary reaction types. The general patterns observed in the previous H-migration reactions are also seen here. Each transition state has a barrier height that is at least 0.8 kcal mol^{-1} lower than for the 8pp reaction in *n*-alkyl radicals (Figure 6F). The 8_4pp and 8_5pp activation energies are both 0.6 kcal mol^{-1} less than those of the 8_2pp and 8_6pp reactions. These differences are again attributable to the differences between the two gauche/anti methyl group shifts in the 4- and 5-methylhept-1-yl radicals compared to only one in the 2- and 6-methylhept-1-yl radicals. Similar to the 1,4 and 1,6 H-migrations involving the 3-methylalkyl radicals, the 8_3pp activation energy is significantly higher than would be predicted by the gauche/anti shifts. However, also similar to the 1,4 and 1,6 H-migrations, the 8_3pp is endothermic, with a ΔH_{rxn} of 0.8 kcal mol^{-1}, which is equal to the difference in barrier height between the 8_3pp and 8_4pp reactions. Given the limited range of ΔH_{rxn} values in the G4 data set for the 1,7 H-migrations, it is not surprising that the reaction enthalpies and activation energies are not well described by an Evans−Polanyi relationship (Figure 7), having an R^2 of 0.25.[47]

For nearly every H-migration reaction, other than the 1,2 H-migrations, the activation energies for reactions with the methyl group positioned within, or immediately outside, the ring structure of the transition state are significantly less than those for the corresponding reactions in *n*-alkyl radicals. This, when combined with the large range of activation energies within each H-migration reaction class and abstraction site type (i.e., primary, secondary, or tertiary), will lead to significant errors in the predicted reaction rates if all reactions of a given type are treated as having the same activation energy or ΔH_{rxn}. Also, the poor fit of the activation energies and reaction enthalpies to an Evans−Polanyi relationship will make the development of automated reaction mechanism programs more difficult.[47]

3.4. Rate Constant. Although the activation energies are generally a good predictor of the relative importance of each reaction in the overall mechanism, other factors such as tunneling and the amount of rearrangement needed to form the transition state (*A*-factor) can also have a significant impact. As a result, although the rate coefficients tend to follow the activation energies, with the rates for the $N_n$tp > $N_n$sp > $N_n$pp, the trends within each of these subgroups do not always follow the expected patterns. Most interesting of all is the observation that, at high temperatures, certain $N_n$sp H-migration reactions have higher rate coefficients than the $N_n$tp reactions for the same *N* value.

For the 1,2 and 1,3 H-migration reactions, the 3_2tp and 4_3tp reactions are significantly higher than the *n*-alkyl radical 3sp and 4sp reactions, by roughly an order of magnitude at 500 K and an factor of 5 at 1000 K (Figure 8A,B). What is interesting is that, although the 3_3sp reactions have activation energies that are higher than for the other 3_nsp reactions, they represent the second fastest 3_nsp reactions at 500 K and the fastest at 1000 K. This suggests that the *A*-factors for the 3_3sp reactions are much higher than for the other reactions (*A*-factors are listed in Table S3 in the Supporting Information). For the 1,3 H-migration reactions, the 3-methylalkyl radicals involve a tertiary site, making the 4_3tp the fastest reaction and obfuscating the *A*-factor effect. The 4_2sp reactions, which have the methyl group in the ring structure of the transition state, have the highest 4_nsp rate coefficients at both 500 and 1000 K. Another interesting trend is observed for the 4_4sp reactions. These reactions have a barrier height similar to that of the 4_2sp reactions but are half as fast as the 4_2sp reactions at 500 K and are the slowest 4_nsp reactions at 1000 K (Figure 8B).

Expanding the transition-state ring by one carbon to produce the 1,4 H-migration reactions results in a significant increase in rate coefficient. The 5_npp reactions in *n*-methylbutyl follow the trends predicted by the activation energies, with the 5_2pp having a higher rate coefficient than the 5_3pp at both 500 and 1000 K (Figure 8C). However, although the 5_2sp, 5_3sp, and 5_5sp reactions all have similar barrier heights, the rate constant for the 5_3sp is approximately twice that of the 5_2sp, which is, for the *n*-methylhexyl radicals, roughly twice that of the 5_5sp. What is surprising is that, at 500 K, the 5_3sp rate coefficients are 45−72% of those of the 5_4tp, and at 1000 K, the 5_3sp reactions are actually faster than the 5_4tp for the *n*-methylhexyl and heptyl radicals. Again, the higher than expected rates for the 3-methylalkyl radicals are the result of significantly higher *A*-factors than for the other *n*-methylalkyl radicals.

For the 1,5 and 1,6 H-migration reactions, there is a significant spread of rate coefficients (Figure 8D,E), with the order of the rates being $N_n$tp > $N_n$sp > $N_n$pp. As a result of this spread, the 5_nsp reactions will be competitive with the 6_npp and 7_npp reactions, but not the 6_nsp or 7_nsp. For both the 1,5 and 1,6 H-migration reactions, the rate coefficients for the N_3sp are

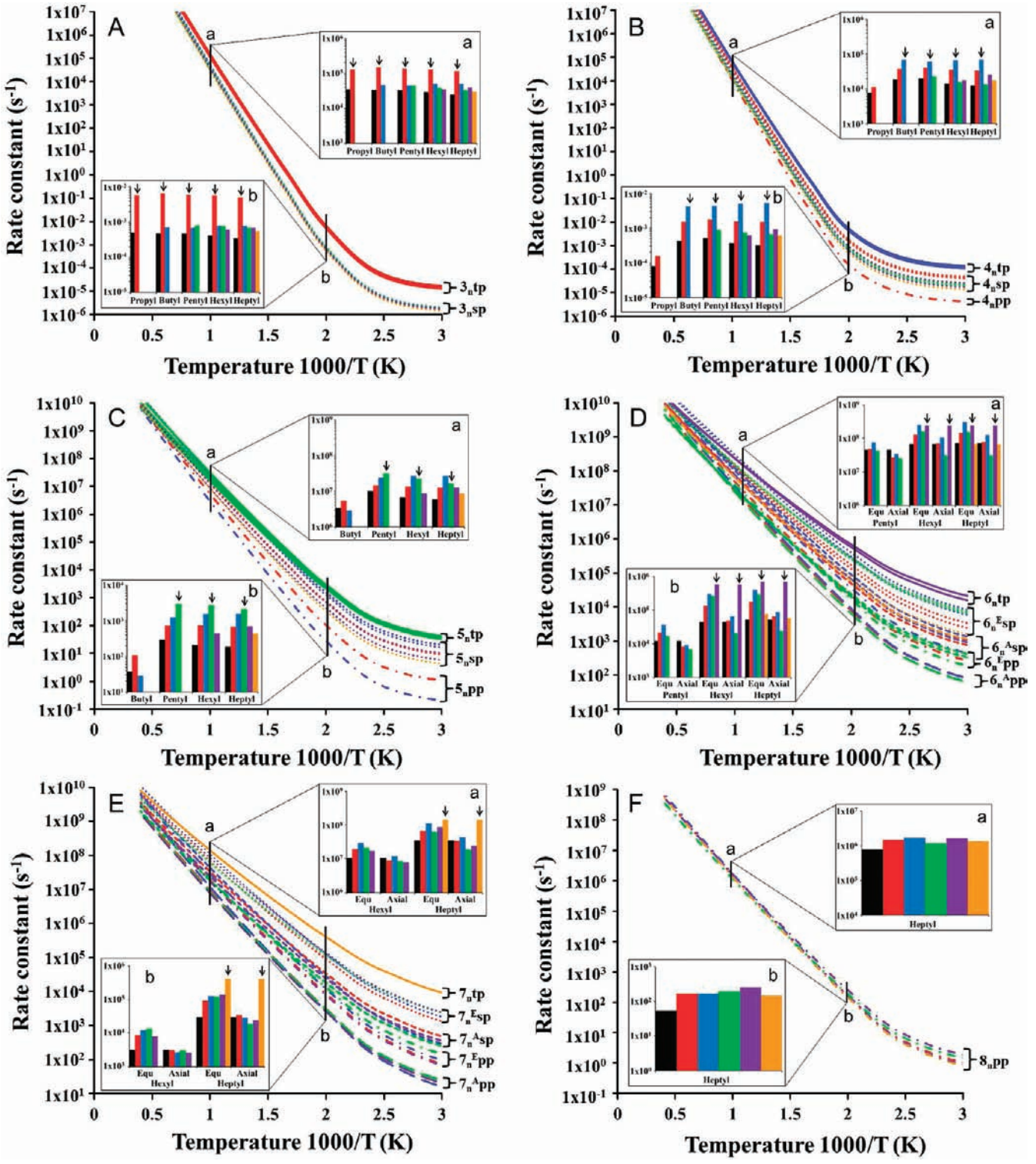

Figure 8. Plot of the G4 rate constants, $k(T)$, for the *n*-methylalk-1-yl radical 1,*n* H-migration reactions, using the Skodje−Truhlar method for predicting the effect of tunneling. The color scheme is the same as used in the respective panels in Figure 6. Each panel has insets showing bar graphs of rate constants at (a) 1000 and (b) 500 K. (A) 1,2 H-migration (arrows in the insets indicate the location of the 3_ntp reactions); (B) 1,3 H-migration (arrows in the insets indicate the location of the 4_ntp reactions); (C) 1,4 H-migration (arrows in the insets indicate the location of the 5_ntp reactions); (D) 1,5 H-migration (arrows in the insets indicate the location of the 6_ntp reactions); (E) 1,6 H-migration (arrows in the insets indicate the location of the 7_ntp reactions); and (F) 1,7 H-migration.

generally the highest of the values for the $N_n$sp reactions, even though the activation energies for these reactions are higher than for either the N_2sp or N_4sp. As before, the higher than expected rate coefficients for the N_3sp reactions are the result of *A*-factors

dx.doi.org/10.1021/ja205516s |*J. Am. Chem. Soc.* 2011, 133, 19110–19124

that are approximately twice those of the other reactions (Table S.3). These high *A*-factor values lead the 3-methylhept-1-yl radical 6_3^Esp reaction to be faster than the 6_5tp, and the 7_3^Esp reaction to be roughly 80% of the 7_6tp, at 1000 K. A comparison of the 1,5 versus the 1,6 H-migration rates shows that, for the *n*-methylhex-1-yl radicals, the 6_nsp and 6_5tp will be the dominant reaction pathways, with the 7_npp reactions contributing roughly 10% toward the end product formation. However, for the *n*-methylhept-1-yl radicals, the 6_nsp and 7_nsp reactions will be competitive with the latter, making up roughly 33−40% of the H-migrations in the combustion mechanism of branched alkyl radicals. For the 6-methylhept-1-yl radical, the 7_6tp will be the dominant pathway, contributing up to 85% and 65% of the branching reactions at 500 and 1000 K, respectively.

Finally, the 1,7 H-migration reactions are much slower, over the entire temperature range, than any of the 1,4 through 1,6 H-migration reactions (Figure 8F). As a result, although they are 2−3 times faster than their *n*-alkyl radical counterparts, the 1,7 H-migration reactions are not expected to contribute significantly to the combustion mechanism of the *n*-methylhept-1-yl radicals. However, based on the observed increases in rate coefficients on going from the $N_n$pp to $N_n$tp reactions, it is possible that the 8_7tp reactions in the 7-methyloct-1-yl radical may contribute toward product formation but will not be the dominant pathway.

In each case, within a particular set of H-migration reactions, the general order of the rate coefficients is $N_n$tp > $N_n$sp > $N_n$pp, as has previously been reported.[30,35] However, within the $N_n$sp and $N_n$pp reactions, the 3-methylalkyl radicals tend to have the highest rate constants, particularly at high temperatures, which is attributable to their *A*-factors being 2 or more times higher than those for other *n*-methylalkyl radicals. The elevated rate coefficients for the 3-methylalkyl radicals are in fact large enough to make the 5_3sp, 6_3^Esp, and 7_3^Esp reactions faster than the corresponding $N_n$tp reactions at high temperatures.

3.5. Methyl Group Chirality and Effect of Axial versus Equatorial Configurations. The rate parameters for hydrogen migration reactions are generally reported on a per hydrogen basis. Experimentally this means that the overall rates for a reaction must be divided by the number of hydrogens at a given abstraction site. The underlying assumption to this practice is that each hydrogen at a given abstraction site has the same kinetic parameters and thus the same rate. However, when transition states are formed, the migrating hydrogen becomes distinguishable from others at the same site. In the case of $N_n$sp reactions, this process introduces chirality to the transition state. For *n*-alkyl radicals, the reactants and products of the H-migration reactions do not contain any chiral sites; thus, each hydrogen migration transition state will contain only one chiral center. Since the ring structure of the transition state is often modeled on cycloalkanes, one can think of two possible potential energy surfaces (PESs) for each hydrogen in an *n*-alkyl radical *N*sp reaction. The first occurs when the remaining alkyl chain takes on an equatorial position; the other occurs when the chain is in the axial position. In a previous study we reported on the relative favorability of these two pathways and determined that the equatorial position is preferred. However, the reactants and products of nearly all *n*-methylalkyl radicals contain at least one chiral site, the tertiary carbon. Thus, in forming a transition state, the $N_n$sp reactions have two chiral sites. For those *n*-methylalkyl radical $N_n$sp H-migration reactions with the methyl group positioned within the ring structure, abstraction of each hydrogen will result in a different directionality of the methyl group, either axial or equatorial. Since the 1,5 and 1,6 H-migrations display a cyclohexane-like ring structure, as described in our previous study on H-migrations in alkyl radicals, the differences in activation energies between the two hydrogens may be as high as 1.8 kcal mol^{-1}, based on 1,3-diaxial interactions in methylcyclohexane.[12,46] The effects of these chiral centers have been exploited for stereoselective synthesis of cyclic structures in organic molecules.[49]

For the 1,5 H-migration reactions, the activation energy for the equatorial, 6_n^Epp and 6_n^Esp configurations are significantly lower than their axial counterparts (Table 2 and Figure 6D). Of particular interest is that the axial configurations have activation energies that are roughly equal to the 6pp and 6sp barrier heights in *n*-alkyl radicals. On the basis of the reaction enthalpies, one would expect the barrier heights for the 6_npp reactions to all be close together, with the 6_2pp being the lowest and the 6_4pp being the highest; for the axial arrangement this is the case. However, if the methyl group is in an equatorial position within the transition-state ring, the 6_3^Epp reaction has the lowest activation energy. For longer methylalkyl radicals, the differences between locations and between an axial and an equatorial arrangement become more prominent.

The axial conformation transition-state barrier heights of the 1,6 H-migration reactions, similar to the 1,5 H-migrations, are significantly higher than those of their equatorial counterparts and, for the most part, are nearly equal to the activation energies of the 1,6 H-migrations in *n*-alkyl radicals. Such behavior is predicted by the gauche/anti effect. During the formation of the 7_n^App and 7_n^Asp transition states, the methyl group rotates from one gauche location to another, leading to the arrangement depicted in Figure 3. When the methylalkyl radical folds to form the transition state, the anti configurations of the reactants rotate into a gauche position and the methyl group which was in one gauche position rotates into the other one. As a result, the 0.8 kcal mol^{-1} reduction in energy on going from gauche to anti that is present in the equatorial reactions is absent from the axial ones. Added to this are the 1,3 diaxial interactions that in cyclohexane add 1.8 kcal mol^{-1} of ring strain, though due to the broader bond angles in the transition states of the H-migration reactions the methyl−axial hydrogen distances are longer, particularly for the 2-methyl- and 5-methylalkyl radicals, in which one of the diaxial interactions occurs across the added distance of the C−H−C bond. The 7_3^App, 7_3^Asp, 7_4^App, and 7_4^Asp reactions, on the other hand, have closer and stronger 1,3 diaxial interactions and, as a result, have significantly higher activation energy barriers than their equatorial counterparts. On the basis of these barriers, the rates of the N_n^App and N_n^Asp reactions would be expected to be similar to the *n*-alkyl *N*pp and *N*sp rates, with the 3-methylheptyl 1,6 H-migrations being significantly lower than the others.

The trends in rate coefficients for the axial arrangement agree with those predicted by the activation energies, except for the H-migrations involving 3-methylalkyl radicals. These radicals have the highest and second highest N_n^Asp rate coefficients at 500 K for the 5_3^Asp and 6_3^Asp reactions, respectively, and both have the highest N_n^Asp rate coefficients at 1000 K. This is again attributable to elevated *A*-factors for the 3-methylalkyl radicals, which, though not as high as their equatorial counterparts, are higher than the *A*-factor values for the other H-migration reactions. For the 1,5 H-migration reactions, the 6_n^Epp and 6_n^Esp rate coefficients are generally 2−6 times higher than those for the 6_n^App and 6_n^Asp reactions, except for the 4-methylhexyl and 4-methylheptyl radicals, in which the 6_4^Esp reactions are

roughly an order of magnitude faster than the 6_4^Asp below 600 K. A similar trend is observed for the 1,6 H-migration reactions, for which the 7_n^Epp and 7_n^Esp are generally 2−6 times faster than the axial form, except for the 7_4^Esp reactions, which are 6−9 times faster than the 7_4^Asp. These differences in rate coefficient can cause significant discrepancies between experimental and computational values, if all hydrogens at a given abstraction site are treated as equal and if rates are reported on a per hydrogen basis. The reason for the difference between these two methods is that experimental studies which use end product concentrations to determine the reaction rates cannot distinguish between the two hydrogens, unless one is replaced with deuterium, since the reactants and products are identical for each. As a result, the experimentally determined rate coefficients for the $N_n$sp reactions would be divided by the number of hydrogens at the abstraction site (two). Since the rates for the N_n^Esp reaction are 2−6 times higher than for the N_n^Asp, this practice would underpredict the rate coefficient for the former by a factor of about 2 and overpredict the latter by up to a factor of 5 for the 6_4^Asp reaction. Computationally, the minimum energy structure corresponds to the equatorial form; if the rate coefficient for this form is reported as the rate coefficient per hydrogen for the $N_n$sp reactions, then the predicted branching contribution of the H-migration reactions would be roughly twice what is observed experimentally. This problem could be exacerbated by the presence of additional methyl groups along the alkyl chain, particularly if they are separated by unbranched carbons, which would increase the 1,3 diaxial interactions. As a result, the use of 2,2,4,4,6,8,8-heptamethylnonane as a surrogate for all branched alkanes in diesel fuels may lead to a significant over- or underprediction of the chain branching effect of H-migration reactions, particularly for branched alkanes with multiple chiral centers.

4. CONCLUSIONS

Branched alkanes are a key component in many alternative fuels. During their combustion and atmospheric decomposition, these fuels are expected to produce methylalkyl radicals. These reactive intermediates can undergo both unimolecular and bimolecular reactions. Of these, the unimolecular H-migration reactions will lead to significant chain branching in the overall reaction mechanisms. This study investigated all of the H-migration reactions available to the 2-methylprop-1-yl through 6-methylhept-1-yl radicals. Reaction enthalpies, activation energies, and rate coefficients are used to study the effect that a methyl group has on the reactivity of alkyl radicals. Due to the geometric similarities of the transition states and cycloalkanes, the effect of the positioning of the methyl group for the 1,5 and 1,6 H-migrations, either axial or equatorial, was also studied.

The barrier heights for H-migration reactions, with the methyl groups located either within or immediately outside the ring, are found to be significantly lower than for similar H-migrations in *n*-alkyl radicals or those reactions with a farther-removed methyl group. The N_2pp, N_{N-2}pp, and N_2sp reactions were generally found to have activation energies ∼0.8−1 kcal mol^{-1} lower in energy than the *n*-alkyl radicals, and ∼0.8−1 kcal mol^{-1} higher than the other reactions with the methyl group located in the transition-state ring. The 0.8 kcal mol^{-1} reduction in activation energy is attributed to the presence of a gauche conformation from the methyl group in the reactants, which shifts to an anti conformation in the transition state. This reduction in energy balances out, to some extent, the shift of the alkyl chain from an anti to gauche conformation when it is forming the transition state. For those reactants in which the methyl group has two gauche interactions, the gauche/anti effect will reduce the barrier height by roughly 1.6 kcal mol^{-1}. Where this was not the case, as with the 3-methylalkyl radicals, the divergence is attributed to an endothermic ΔH_{rxn} value which, when summed with the expected −1.6 kcal mol^{-1} from two gauche−anti shifts, yields theoretical values that are very similar to those determined computationally. However, for the axial transition-state conformations, the methyl group shifts from one gauche location to the other, resulting in no significant net reduction in barrier height. As a result, the activation energies for the 1,5 and 1,6 H-migration axial reactions are roughly equal to those for the corresponding reactions in the *n*-alkyl chain.

Although the general order of rate coefficients is $N_n$tp > $N_n$sp > $N_n$pp, as has previously been reported, within the $N_n$sp and $N_n$pp reactions the 3-methylalkyl radicals tend to have the highest rate constants, particularly at high temperatures. This trend corresponds to the *A*-factors being 2 or more times higher for the 3-methylalkyl radicals than for the other *n*-methylalkyl radicals. Surprisingly, the elevated rate coefficients for the 3-methylalkyl radicals are large enough to make the 5_3sp, 6_3^Esp, and 7_3^Esp reactions faster than their corresponding $N_n$tp reactions at high temperatures. A comparison between the various H-migrations suggests that the 1,5 H-migrations are the dominant H-migration reaction for all *n*-methylalkyl radicals, except for the 6-methylhept-1-yl radical, where the 7_6tp is faster than the 6_6sp reaction. Although the 1,6 H-migration reactions are not the dominant pathway, they will still be competitive with the 1,5 and may be responsible for as much as 30−40% of the chain branching reactions for the heptyl and larger *n*-methylalkyl radicals.

Due to the differences between the axial and equatorial methyl group positions, which in the $N_n$sp reactions are dictated by which hydrogen is abstracted, the treatment of each hydrogen on a given abstraction site as equivalent will result in the over -or underestimation of the reaction rate for each hydrogen. Furthermore, the secondary effects of the methyl group on the barrier heights, through the gauche/anti shifts, mean that the treatment of the $N_n$sp reactions as having the same rate parameters as *N*sp reactions in *n*-alkyl radicals will lead to significant errors in the estimated rate coefficients.

To further assess the validity of the anti/gauche effect on branched alkyl radicals, future studies, both experimental and computational, should be conducted on polymethylalkyl radicals. Of particular interest would be an experimental comparison between 3-methylhexane and 3,3-dimethylhexane, the latter of which should have a 1,5 H-migration rate that is twice that of the former, based on the differences between the axial and equatorial rates reported here, which will be absent from the 3,3-dimethylhexyl radical. Also, dimethylalkyl radical *R*,*R* and *R*,*S* diastereomers, depending on the location of the methyl groups, should exhibit significantly different H-migration rates and, as a result, different relative end product concentrations.

■ ASSOCIATED CONTENT

Supporting Information. Complete ref 37; tabulated frequencies and rotational constants for reactants, products, and transition states; tabulated Arrhenius pre-exponential factors for the forward and reverse reactions; tabulated tunneling transmission coefficients determined using the Skodje−Truhlar

and the Wigner methods; tabulated heat capacities; and Cartesian coordinates for reactants, products, and transition states in this study. This material is available free of charge via the Internet at http://pubs.acs.org.

AUTHOR INFORMATION

Corresponding Author
francisc@purdue.edu

ACKNOWLEDGMENT

We thank the Purdue Rosen Center for Advanced Computing for their assistance with providing and maintaining the computational resources used for this study. Background art is used with the permission of Alexej Bodemer.

REFERENCES

(1) Eliseev, O. L. *Russ. J. Gen. Chem.* **2009**, *79*, 2509–2519.
(2) Dry, M. E. *J. Chem. Technol. Biotechnol.* **2002**, *77*, 43–50.
(3) Westbrook, C. K.; Smith, P. J. *Basic Research Needs for Clean and Efficient Combustion of 21st Century Transportation Fuels*; Lawrence Livermore National Laboratory, Livermore, CA, 2006.
(4) Simmie, J. M. *Prog. Energy Combust. Sci.* **2003**, *29*, 599–634.
(5) Pitz, W. J.; Mueller, C. J. *Prog. Energy Combust. Sci.* **2011**, *37*, 330–350.
(6) Curran, H. J.; Gaffuri, P.; Pitz, W. J.; Westbrook, C. K. *Combust. Flame* **1998**, *114*, 149–177.
(7) Curran, H. J.; Gaffuri, P.; Pitz, W. J.; Westbrook, C. K. *Combust. Flame* **2002**, *129*, 253–280.
(8) Westbrook, C. K.; Pitz, W. J.; Herbinet, O.; Curran, H. J.; Silke, E. J. *Combust. Flame* **2009**, *156*, 181–199.
(9) Watkins, K. W.; O'Deen, L. A. *J. Phys. Chem.* **1971**, *75*, 2665–2672.
(10) McGivern, W. S.; Awan, I. A.; Tsang, W.; Manion, J. A. *J. Phys. Chem. A* **2008**, *112*, 6908–6917.
(11) Awan, I. A.; McGivern, W. S.; Tsang, W.; Manion, J. A. *J. Phys. Chem. A* **2010**, *114*, 7832–7846.
(12) Davis, A. C.; Francisco, J. S. *J. Phys. Chem. A* **2011**, *115*, 2966–2977.
(13) Endrenyi, L.; Le Roy, J. D. *J. Phys. Chem.* **1966**, *70*, 4081–4084.
(14) Watkins, K. W. *J. Am. Chem. Soc.* **1971**, *93*, 6355–6359.
(15) Watkins, K. W.; Lawson, D. R. *J. Phys. Chem.* **1971**, *75*, 1632–1640.
(16) Sefton, V. B.; Le Roy, D. J. *Can. J. Chem.* **1956**, *34*, 41–53.
(17) Miyoshi, A.; Widjaja, J.; Yamauchi, N.; Koshi, M.; Matsui, H. *Proc. Combust. Inst.* **2002**, *29*, 1285–1293.
(18) Tsang, W.; Walker, J. A.; Manion, J. A *27th Int. Symp. Combust.* **1998**, 135–142.
(19) Tsang, W.; Walker, J. A.; Manion, J. A *Proc. Combust. Inst.* **2007**, *31*, 141–148.
(20) Babushok, V. I.; Tsang, W. *J. Propul. Power* **2004**, *20*, 403–414.
(21) Tsang, W.; McGivern, S.; Manion, J. A. *Proc. Combust. Inst.* **2009**, *32*, 131–138.
(22) Yamauchi, N.; Miyoshi, A.; Kosaka, K.; Koshi, M.; Matsui, H. *J. Phys. Chem. A* **1999**, *103*, 2723–2733.
(23) Zheng, J. J.; Truhlar, D. G. *J. Phys. Chem. A* **2009**, *113*, 11919–11925.
(24) Viskolcz, B.; Seres, L. *React. Kinet. Catal.* **2009**, *96*, 245–262.
(25) Viskolcz, B.; Lendvay, G.; Kortvelyesi, T.; Seres, L. *J. Am. Chem. Soc.* **1996**, *118*, 3006–3009.
(26) Sirjean, B.; Wang, H.; Tsang, W. Presented at the 6th U.S. National Combustion Meeting Ann Arbor, MI, 2009.
(27) Ratkiewicz, A.; Bankiewicz, B.; Truong, T. N. *Phys. Chem. Chem. Phys.* **2010**, *12*, 10988–10995.
(28) Jitariu, L. C.; Jones, L. D.; Robertson, S. H.; Pilling, M. J.; Hillier, I. H. *J. Phys. Chem. A* **2003**, *107*, 8607–8617.
(29) Jitariu, L. C.; Wang, H.; Hillier, I. H.; Pilling, M. J. *Phys. Chem. Chem. Phys.* **2001**, *3*, 2459–2466.
(30) Hayes, C. J.; Burgess, D. R., Jr. *J. Phys. Chem. A* **2009**, *113*, 2473–2482.
(31) Matheu, D. M.; Green, W. H., Jr.; Grenda, J. M. *Int. J. Chem. Kinet.* **2003**, *35*, 95–119.
(32) Viskolcz, B.; Lendvay, G.; Seres, L. *J. Phys. Chem. A* **1997**, *101*, 7119–7127.
(33) Barker, J. R.; Ortiz, N. F. *Int. J. Chem. Kinet.* **2001**, *33*, 246–261.
(34) Bankiewicz, B.; Huynh, L. K.; Ratkiewicz, A.; Truong, T. N. *J. Phys. Chem. A* **2009**, *113*, 1564–1573.
(35) Benson, S. W. *Thermochemical Kinetics*, 2nd ed.; Wiley: New York, 1976.
(36) Hardwidge, E. A.; Larson, C. W.; Rabinovitch, B. S. *J. Am. Chem. Soc.* **1970**, *92*, 3278–3283.
(37) Frisch, M. J.; et al. *Gaussian09*, Rev. A.1; Gaussian, Inc.: Wallingford, CT, 2009.
(38) Ochterski, J. W.; Pererson, G. A.; Wiberg, K. B. *J. Am. Chem. Soc.* **1995**, *117*, 11299–11308.
(39) Curtiss, L. A.; Redfern, P. C.; Raghavachari, K. *J. Chem. Phys.* **2007**, *126*, 12.
(40) Davis, A. C.; Francisco, J. S. *J. Phys. Chem. A* **2010**, *114*, 11492–11505.
(41) Ochterski, J. W.; Pererson, G. A.; Montgomery, J. A., Jr. *J. Chem. Phys.* **1996**, *104*, 2598–2619.
(42) Curtiss, L. A.; Raghavachari, K.; Trucks, G. W.; Pople, J. A. *J. Chem. Phys.* **1991**, *94*, 7221–7230.
(43) Curtiss, L. A.; Redfern, P. C.; Raghavachari, K. *J. Chem. Phys.* **2007**, *126*, 084108.
(44) Cohen, N. *J. Phys. Chem.* **1992**, *96*, 9052–9058.
(45) Sumathi, R.; Carstensen, H. H.; Green, W. H. *J. Phys. Chem. A* **2001**, *105*, 6910–6925.
(46) Carey, F. A., Sundberg, R. J. *Advanced Organic Chemistry Part A: Structure and Mechanisms*, 3rd ed.; Plenum Press: New York, 1990.
(47) Evans, M. G.; Polanyi, M. *Trans. Faraday Soc.* **1938**, *34*, 11–24.
(48) Larson, C. W.; Chua, P. T.; Rabinovitch, B. S. *J. Phys. Chem.* **1972**, *76*, 2507–2517.
(49) Bar, G.; Parsons, A. F. *Chem. Soc. Rev.* **2003**, *32*, 251–263.
(50) *Computational Chemistry Comparison and Benchmark DataBase*; National Institute of Standards and Technology, http://cccbdb.nist.gov/ (accessed 5/17/2011).